

Glass–ceramic matrix composites with high oxidation embrittlement resistance

K. P. GADKAREE

Corning Inc., Sullivan Park, Corning NY 14831, USA

A new concept is introduced to minimize the oxidation embrittlement problem exhibited by Nicalon fibre-reinforced glass–ceramic matrix composites. A small amount of glass is added to the matrix and deforms at temperatures of interest to prevent microcrack formation. The graphitic interphase is thus shielded from an oxidative environment. The composites fabricated with the glass-doped matrices show excellent room- and elevated-temperature strengths and withstand high stresses at elevated temperatures in air for greater than 100 h without any deterioration in properties. The modulus of the glass–ceramic phase, the stiffness percentage of dopant glass and the process temperature were found to affect composite properties significantly.

1. Introduction

Glass and glass–ceramic matrix composites reinforced with continuous Nicalon® silicon oxycarbide fibres have been studied extensively for high-temperature aerospace applications [1–3]. In such composites the matrix has a significantly lower failure strain (0.1%) compared to the fibre (>1%). This difference in failure strains results in matrix microcracking at a strain much lower than the ultimate failure strain of the composite. Beyond the microcrack point the composite consists of a severely cracked matrix held together by the fibres. The matrix microcrack stress is only about 30 to 50% of the ultimate strength of the composite. Composites of Nicalon fibre and a glass or glass–ceramic matrix derive their strength and toughness from an *in situ* graphitic layer that develops during the processing of the composite. At temperatures where the oxidation rate of the graphitic layer is slow, the composites exhibit tough failure. The graphitic layer is not exposed to an oxidizing environment below the microcrack point. Above the microcrack point, however, the graphitic layer is subject to oxidation. At high temperatures (~900–1000°C) the graphitic interface oxidizes very quickly and the composite fails in a brittle manner [4]. Since a gradual failure mode for the composite is essential for high-temperature structural applications, this problem has to be solved.

One way to alleviate the problem is to increase the microcrack stress substantially. This can be achieved by hybridization [5]. Although significant improvements are obtained in microcrack stress and strain, the composite failure remains brittle at elevated temperatures. This occurs because the underlying cause of embrittlement, i.e. oxidation of the graphitic layer, is not addressed. Another proposed solution is to replace the graphitic interface which oxidizes quickly with an oxidation-resistant weak interface. Oxidation-resistant interlayers such as boron nitride [6] and

oxide layers obtained from mica glass–ceramics [7] have been evaluated with various degrees of success. These approaches, wherein the chemistry of the interface is changed significantly, may be termed “chemical” approaches to the solution of the oxidation-embrittlement problem.

In this paper a novel solution for the oxidation-embrittlement problem is described. In this approach the interface is not chemically modified but protected at high temperatures by a matrix which has a higher strain to failure than the fibre. The strength and toughness of the composite are still derived from the same weak graphitic interface. The approach is based on mechanistic principles of composite behaviour.

1.2. The concept

To eliminate oxidation embrittlement the graphitic interface must be protected from an oxidizing environment. This protection is afforded by the matrix if microcracking of the matrix is avoided. Microcracking of the matrix can be prevented if the failure strain of the matrix is higher than the failure strain of the fibre. Such a situation exists in polymer-matrix composites, for example where the polymeric matrix has a higher failure strain than the fibre. It is well known that glass–ceramic matrices have significantly lower failure strains (~0.1%) compared to those of fibres (~1%). A glass–ceramic matrix with a higher failure strain than that of the fibre can be obtained, at least at high temperatures, by doping the refractory matrix with a small amount of glass. The glass will allow the matrix to deform without microcracking at temperatures of interest. Since the graphitic interface is not exposed to the oxidative environment, embrittlement of the interface does not occur.

The dopant glass must satisfy the following requirements to be useful. The glass should be refractory (i.e. high viscosities at temperatures of interest), while at

the same time softening at low temperatures (600 to 700 °C) to provide oxidation resistance at these low temperatures. In effect the glass should have a relatively flat viscosity–temperature curve. The glass must also be chemically compatible with the glass–ceramic phase to maintain a stable matrix system at high temperatures.

Because an addition of glass results in increased plasticity at elevated temperatures, a lower creep resistance and lower interlaminar shear strength could result. This problem is solved by the addition of high-modulus silicon carbide whiskers to the doped matrix. The whisker-reinforced matrix has better load transfer characteristics because of increased modulus, better creep resistance and better off-axis properties. It is known [8] that as the matrix becomes more plastic at high temperatures, the effectiveness of the whiskers as reinforcement decreases. The whisker-reinforced matrix, however, should have a higher creep resistance than the unreinforced matrix. Selection of the dopant glass and the glass–ceramic matrix based on the criteria mentioned above are described in the following section.

2. Experimental procedure

2.1. Materials

Borosilicate glasses compared to other glasses are known to have the characteristic of a flat viscosity curve. The borosilicate glasses are greatly stable and refractory. A potassium borosilicate glass (Corning 7761) typifies the desired dopant, and was chosen as the primary dopant candidate. This glass has an annealing point of 510 °C, strain point at 438 °C, softening point at 820 °C and working point at 1300 °C. This glass should thus deform and blunt cracks, thereby providing oxidation protection of the C-rich interface over an extended temperature range. Barium-stuffed cordierite was chosen as the glass–ceramic matrix because it has a better thermal expansion match with the 7761 glass and has a higher modulus (131 GPa) compared to that (96 GPa) of other successful anorthite-based glass–ceramics. This higher modulus of the matrix allows better load transfer to the whiskers [8].

Arco SC-9 whiskers from ACMC (Greer, South Carolina) and Nicalon NLM202 oxycarbide fibres from Nippon Carbon were used in all experiments.

2.2. Processing

All glasses were melted in platinum crucibles at 1600 °C. The compositions contain appropriate levels of dopant glass constituents. Patties were poured from the glasses, and subsequently were then ground to 10 µm mean particle size. The whiskers were mixed at 10 wt % level with the glass powder in isopropanol by ball-milling. The mixture was filtered and dried. The Nicalon fibres were then impregnated with the glass powder and whisker mixture using a polymeric binder system. The uniaxial prepreps were stacked; the binder was burned off in air, and then hot-pressed in graphite dies at temperatures between 1000 and 1300 °C.

2.3. Property evaluation

Samples for mechanical properties were 75 mm × 4 mm × 2 mm. Mechanical property evaluations included the following:

(i) Fast-fracture strength measurement at room temperature and elevated temperature (up to 1200 °C) in air. To identify if the embrittlement phenomenon was present.

(ii) Static fatigue experiments, obtained in air in the temperature range 800–1000 °C at stress levels significantly above the microyield stress for extended periods of time. The specimens which survived the static fatigue test were retested at room temperature to evaluate and compare their properties with the properties obtained in the as-pressed condition.

(iii) Tension–tension cyclic fatigue tests, obtained in air at 1000 °C at 1 Hz frequency on selected composites. For these experiments the maximum stress level was significantly above the microyield stress. The selected composites survived 10⁶ cycles without any deterioration in properties.

This paper describes the results of the first two tests. The tension–tension cyclic fatigue tests have also been completed and the results will be published separately.

3. Results and discussion

3.1. Matrix properties

Incorporation of dopant glass into the glass–ceramic matrix can be achieved in two ways. The glass and the glass–ceramic may be separately melted, ground to powder, and then mixed by ball-milling or another technique. On the other hand, the glass and glass–ceramic can be melted together as a single composition and then the glass–ceramic may be nucleated and crystallized out with the glass at the grain boundaries. The second method is preferred because a uniform distribution of the glass in the matrix will result. Also, if the glass–ceramic can separate out and crystallize apart from dopant glass, reaction between the dopant glass and the glass–ceramic, which might cause long-term stability problems, can be avoided. In all the compositions herein, the second approach was the chosen methodology. A glass of appropriate mixed composition was melted, and clear glass patties were obtained. Samples of glass patties were cerammed and analysed by X-ray diffraction to determine the crystal phase assemblage. For anorthite, cordierite and anorthite + cordierite based compositions doped with various borosilicate glasses, the desired crystal phases always formed on ceramming. This suggests that there may be no long-term stability issues with these systems.

The percentage of dopant glass in the matrix was critical to oxidation-embrittlement resistance. As noted earlier, a high level of glass would result in a high level of plasticity in the matrix, resulting in poor load transfer and lower creep resistance of the composite. Too low a glass content would result in the microcracks not being blunted and would allow oxidation embrittlement. Similar arguments may be advanced regarding the stiffness of the dopant glass for a

given dopant glass percentage in the matrix. A very stiff glass at a given temperature may not cause blunting of the microcracks, while a very fluid glass may not have enough load transfer ability or creep resistance.

Glass levels of 2.5, 5 and 7.5% by weight of the matrix glass were evaluated initially. The effect of stiffness variation of the glass was also studied by removing K_2O from the glass composition and/or varying the SiO_2/B_2O_3 ratio in the glass. Experiments utilized the Ba cordierite matrix.

Matrix phase stability was characterized after exposure to elevated temperatures for 100 h. For each composition, glass powder bars were sintered in air and exposed at 1000, 1100 and 1200 °C for 1, 10 and 100 h in sequence. X-ray diffraction patterns were then obtained for each of these bars to determine whether significant phase changes had occurred. No significant differences were observed, indicating that the phases are stable over the time and temperature range studied.

Transmission electron micrographs of thin films of the systems were also obtained. Initial attempts to obtain replica micrographs did not yield useful results. The thin-film technique did give good micrographs of the specimens. Fig. 1 shows a transmission micrograph for the 5 wt % glass-doped system. Cordierite grains with the glass at the grain boundaries are clearly seen. As expected, more glass is observed at the grain boundaries as the glass doping level was increased.

The modulus of the matrices was also measured by a sonic resonance technique up to 1200 °C for each of the matrix systems. For the 2.5 wt % doped glass system, the modulus varied from 133 GPa at 25 °C to 81 GPa at 1200 °C. The modulus changed from 128 to 70 GPa for the 5 wt % doped system and from 122 to 66 GPa for the 7.5 wt % doped system over the same temperature range. With increasing glass doping level there is thus a small decrease in the modulus of the system at room temperature as well as at elevated temperatures. Fig. 2 shows the modulus data for the

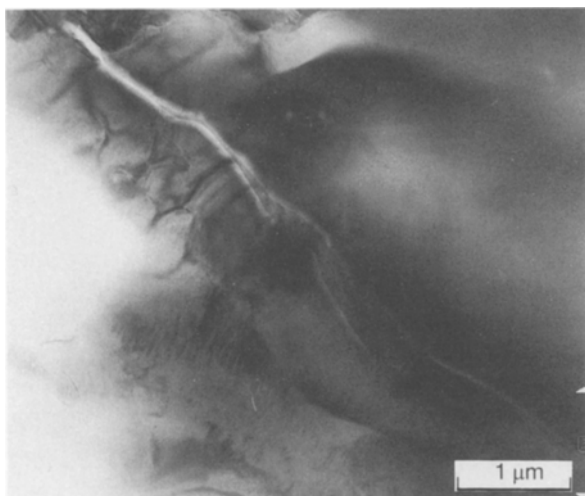


Figure 1 TEM replica of 5 wt % glass-doped matrix (cordierite grains and glass at grain boundaries).

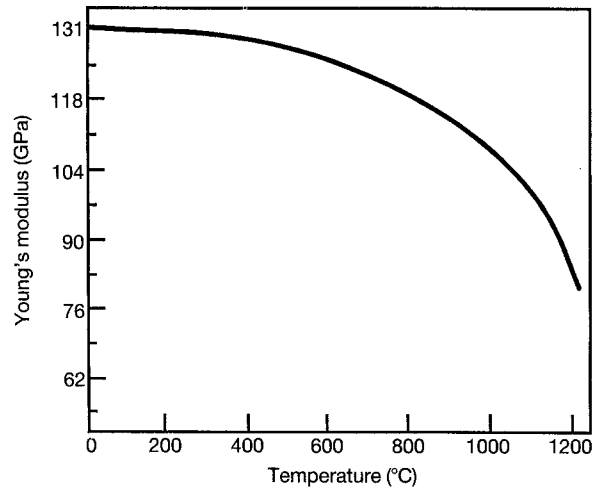


Figure 2 Modulus of 2.5 wt % glass-doped matrix as a function of temperature.

2.5 wt % glass-doped system as a function of temperature.

Thermal expansion and differential thermal analysis (DTA) data were also obtained on the three matrices. The thermal expansion from 25 to 900 °C is about the same for all the matrices. The thermal expansion coefficient is 2.35, 2.5 and 2.39 p.p.m °C⁻¹ for 2.5, 5 and 7.5 wt % glass-doped samples, respectively. DTA data do not show any significant differences, with strong crystallization peaks appearing at 1025 °C. The crystals melt at temperatures of 1410 to 1420 °C.

3.2. Composite properties

3.2.1. Flexural strength

For glass-ceramic matrix composites, determination of the optimum process temperature is important since the properties of the composites vary substantially as a function of process temperature. Composites were fabricated at 1200, 1250 and 1300 °C, and the flexural strengths were measured as a function of temperature to determine the optimum process temperature for each composition.

Initially the composite properties increased with the hot-pressing temperature. Tables I to III show the properties of the 2.5, 5 and 7.5 wt % glass-doped composites, respectively. As Table I shows, the ultimate failure strengths are high at 25, 1000 and 1200 °C for the 2.5 wt % glass-doped system from all fabrication temperatures. However, the ultimate failure strengths are highest at 25 and 1000 °C for the 1250 °C fabrication temperature. At the 1200 °C test temperature, the ultimate failure strength for the composite processed at 1250 °C is about the same as at other process temperatures. The ultimate failure strain at room temperature is highest for the composite processed at 1250 °C. At 1000 °C, however, the ultimate failure strain for the composite processed at 1200 °C is highest (0.83%). The 1250 °C process temperature results in 0.71% ultimate failure strain at 1000 °C, and the 1300 °C process temperature results in 0.60% ultimate failure strain at 1000 °C. At 1200 °C the

TABLE I Effect of hot-press temperature on flexural properties (2.5 wt % glass doping)

Hot-press temperature (°C)	Test temperature (°C)	σ_{MY} (MPa)	ϵ_{MY} (%)	σ_{ULT} (MPa)	ϵ_{ULT} (%)
1200	25	379	0.23	628	0.47
	1000	90	0.09	600	0.83
	1200	51	0.07	462	1.00
1250	25	421	0.28	787	0.87
	1000	145	0.14	628	0.71
	1200	62	0.09	460	0.99
1300	25	400	0.25	683	0.51
	1000	138	0.13	538	0.60
	1200	62	0.09	483	0.90

ultimate failure strain is 1, 0.99 and 0.90% for samples with the process temperatures of 1200, 1250 and 1300 °C, respectively.

The microcrack stresses and strains at 25 and 1200 °C, are about the same for all the process temperatures. At 1000 °C, however, the microcrack stress and strain are significantly higher for composites processed at 1250 and 1300 °C compared to the composite processed at 1200 °C. ("Microcrack" is a term used to conform with earlier usage of the word. Actually "microyield" or "elastic limit" may be more appropriate for these composites at elevated temperatures.) A comparison of the properties suggests 1250 °C as the optimum process temperature.

Table II summarizes the properties of the composites with 5 wt % glass loading. The ultimate failure strength obtained at 25 °C is highest for the sample with a 1300 °C process temperature. The average ultimate failure strain (0.88%) is also highest for the 1300 °C process temperature at 25 °C. As the process temperature decreases from 1300 to 1250 to 1200 °C, the ultimate failure stress and strain decrease from 876 MPa/0.88% to 600 MPa/0.5%. The highest ultimate failure strains and ultimate strengths at elevated temperature, i.e. 1000 and 1200 °C, were obtained with composites processed at 1250 °C. At 1000 °C the ultimate failure stress obtained with composites processed at 1200 and 1250 °C is the same, i.e. 600 MPa.

TABLE II Effect of hot-press temperature on properties (5 wt % glass doping)

Hot-press temperature (°C)	Test temperature (°C)	σ_{MY} (MPa)	ϵ_{MY} (%)	σ_{ULT} (MPa)	ϵ_{ULT} (%)
1200	25	380	0.25	600	0.50
	1000	90	0.09	600	0.8
	1200	46	0.08	421	1.06
1250	25	400	0.26	760	0.71
	1000	138	0.15	600	0.76
	1200	55	0.08	524	1.3
1300	25	373	0.24	876	0.88
	1000	117	0.13	545	0.7
	1200	59	0.09	400	0.9

The microyield stresses and strains at the test temperatures are not significantly different as a function of process temperature. The 1250 °C process temperature appears to generate the optimum balance of properties for this system as in the case of the 2.5 wt % glass-doped system.

Fig. 3 shows the fracture surface of the 5 wt % glass-doped system tested at 25 °C. The fracture is of fibrous, woody type. A similar fracture morphology is seen at 1000 °C, but with reduced pull-out lengths (Fig. 4). At 1200 °C the fracture is fibrous with long pull-out lengths (Fig. 5).

Table III summarizes the properties of the 7.5 wt % glass-doped system. Ultimate failure strains and stresses with values of 966, 862 and 821 MPa and 1.03, 1.00 and 0.97%, respectively, at 25 °C are high at all process temperatures. Properties for the composite processed at 1200 °C are significantly better at test temperatures of 1000 and 1200 °C than those for the composite processed at 1300 °C. The 1250 °C process temperature results in a microyield point of 131 MPa, as against 52 MPa for the process temperature of 1200 °C. For this reason 1250 °C was chosen as the optimal process temperature.

Tables IV to VI indicate room- and elevated-temperature MORs of the composite systems processed at 1250 °C. Data were obtained at temperatures from 25

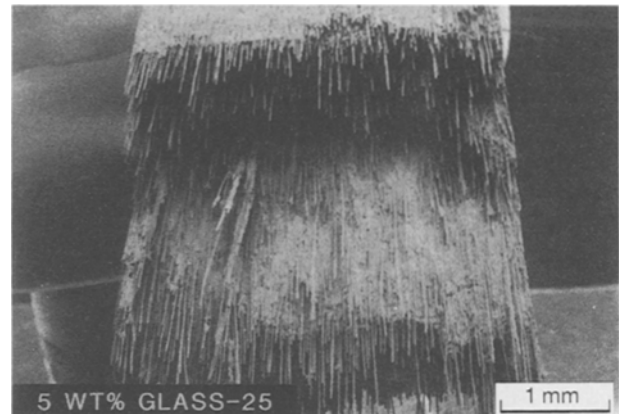


Figure 3 Fracture surface of 5 wt % glass-doped matrix; composite tested at 25 °C.

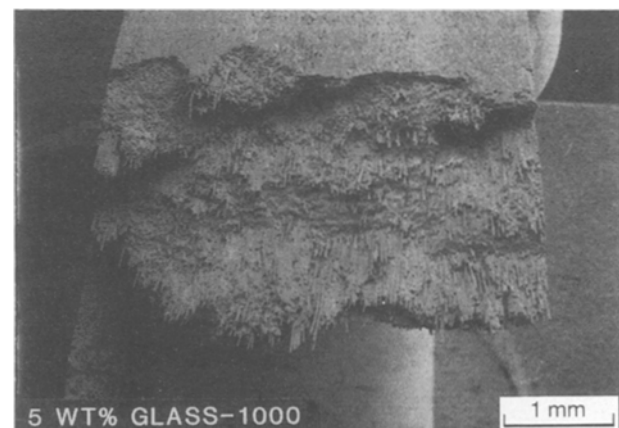


Figure 4 Fracture surface of 5 wt % glass-doped matrix; composite tested at 1000 °C in air.

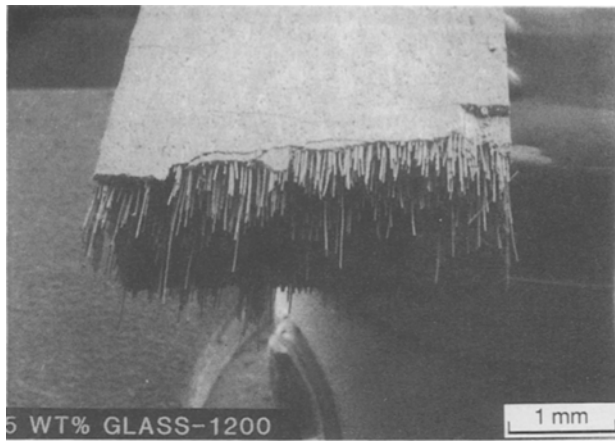


Figure 5 Fracture surface of 5 wt % glass-doped matrix; composite tested at 1200 °C in air.

TABLE III Effect of hot-press temperature on properties (7.5 wt % glass doping)

Hot-press temperature (°C)	Test temperature (°C)	σ_{MY} (MPa)	ϵ_{MY} (%)	σ_{ULT} (MPa)	ϵ_{ULT} (%)
1200	25	400	0.26	966	1.03
	1000	52	0.06	745	1.00
	1200	48	0.09	414	1.08
1250	25	400	0.26	863	1.00
	1000	131	0.13	731	0.89
	1200	63	0.09	449	1.2
1300	25	366	0.24	821	0.97
	1000	124	0.14	620	0.99
	1200	48	0.08	330	0.82

TABLE IV Flexural strength as a function of temperature (2.5 wt % glass doping)

Test temperature (°C)	σ_{MY} (MPa)	ϵ_{MY} (%)	σ_{ULT} (MPa)	ϵ_{ULT} (%)
25	421	0.28	787	0.87
500	450	0.21	876	0.87
600	450	0.27	848	0.82
700	448	0.36	745	0.72
800	435	0.36	740	0.50
900	449	0.40	731	0.70
1000	145	0.14	628	0.71
1200	62	0.09	469	0.99
1250	40	0.08	380	1.23

to 1200 °C. In Table IV (data for the 2.5 wt % glass system), the ultimate strengths remain high up to 1000 °C. At 1200 °C the strength declines to 469 MPa. Ultimate failure strains remain above 0.7% at all temperatures except at 800 °C, where the ultimate failure strain is 0.5%. The ultimate strength is also somewhat lower, i.e. 566 MPa, at 800 °C. At 700 and 900 °C, ultimate strengths and stresses are significantly higher. The microcrack stress or microyield point (depending on temperature) remains high up to

900 °C. The microyield point is 145 MPa at 1000 °C and 62 MPa at 1200 °C.

Table V outlines the properties of the 5 wt % glass-doped system. High ultimate strengths and failure strains are seen at all temperatures, except at 800 °C where the ultimate failure strain is 0.47%. The microcrack or yield points are high up to 900 °C, while the microyield point declines at 1000 °C and above.

Table VI shows the MORs for the 7.5 wt % glass-doped system. Ultimate strains and ultimate strengths are high up to 1000 °C with no decline in properties at intermediate temperatures. The microcrack or microyield stresses also remain high up to 800 °C, beyond which there is a gradual decline as expected. A comparison of data in Tables IV, V and VI does not show any significant property differences up to 1200 °C between the three glass doping levels. At 1250 °C, however, differences appear among the systems with ultimate strengths of 380, 283 and 250 MPa for 2.5, 5 and 7.5 wt % glass-doped systems, respectively.

3.2.2. Static fatigue experiments

Static fatigue experiments were carried out on the specimens at elevated temperatures in four-point flexure with 75 mm support span and 19 mm load span. In each case specimens were loaded significantly above the microyield point. All three glass-doped systems were evaluated.

TABLE V Flexural strength as a function of temperature (5 wt % glass doping)

Test temperature (°C)	σ_{MY} (MPa)	ϵ_{MY} (%)	σ_{ULT} (MPa)	ϵ_{ULT} (%)
25	400	0.26	760	0.71
500	359	0.28	760	0.71
600	386	0.28	760	0.69
700	434	0.33	689	0.63
800	434	0.38	538	0.47
900	262	0.26	538	0.61
1000	140	0.15	600	0.76
1200	55	0.08	524	1.2
1250	22	0.06	283	1.29

TABLE VI Flexural strength as a function of temperature (7.5 wt % glass doping)

Test temperature (°C)	σ_{MY} (MPa)	ϵ_{MY} (%)	σ_{ULT} (MPa)	ϵ_{ULT} (%)
25	400	0.26	790	0.56
500	365	0.25	759	0.66
600	400	0.24	724	0.64
700	420	0.33	759	0.61
800	359	0.29	720	0.57
900	263	0.25	745	0.79
1000	130	0.13	731	0.89
1200	62	0.09	448	1.2
1250	48	0.11	200	0.67

3.2.2.1. *Experiments at 1000 °C.* Initial experiments were carried out at 1000 °C. The specimens tested were the ones processed at 1250 °C hot-pressing temperature. Microyield points for the three systems processed at this temperature were 138 ± 7 MPa. Static fatigue experiments were then undertaken at 276, 345 and 415 MPa.

For the 2.5 wt % glass-doped system there were no failures at any load for 100 h in air at 1000 °C, and specimens were removed from the test rig at the end of the 100 h period. These specimens were then tested in flexure at 25 °C to measure the residual strength. There was no change in mechanical properties such as ultimate strength, ultimate strain or microcrack stress or strain in any case. The results are summarized in Table VII. The glass-doped matrix specimens can be loaded above the microyield point for long periods of time at elevated temperatures with no degradation in mechanical properties. This result shows substantial improvement in oxidation-embrittlement property compared to that for conventional non-glass-doped systems where failure occurs immediately as the stress exceeds the microcrack stress.

For 5 wt % glass-doped specimens the experiments were repeated at loads of 276, 345, and 415 MPa at 1000 °C. At 276 and 345 MPa static load, specimens survived for 100 h without failure. The flexural properties of the specimen after the static fatigue experiments did not show any degradation. At 415 MPa load there was again no failure for 100 h. However, a small shear crack was noted in the specimen below one of the load points at the end of the experiment. The residual strength of this specimen declined from 794 to 656 MPa on testing at room temperature. Calculation of the shear stresses for the specimen geometry and testing geometry indicated that the maximum shear stress was below the load points. It is thought that the shear crack resulted when the shear stress of 31 MPa exceeded the interlaminar shear strength of the specimen. Failures of the specimen will then take place if the interlaminar shear strength of the specimen is exceeded. The interlaminar shear strength can be increased by incorporating higher aspect-ratio whiskers or possibly by introducing stiffer glass dopants. For the 7.5 wt % glass-doped system, similar

results were obtained. No failures occurred at any of the load levels, and all composites retained their as-pressed properties.

3.2.2.2. *Experiments at 900 °C.* Table VIII shows the results of 900 °C static fatigue tests on the three composite systems. The microyield point stress for the 7.5 wt % glass-doped system is 262 MPa. The static fatigue experiment was carried out at 415 MPa without failure for 108 h, and the specimen retained its strength after the experiment.

For the 5 wt % system at 345 MPa load there was no failure for 126 h, at which time the test was terminated. The retained strength of the specimen was 828 MPa with an ultimate failure strain of 0.77%. However, at 415 MPa load the specimen failed in a tensile/shear mode after 24 h. Thus, the specimen in the 5 wt % system survived loads above the microyield point (345 MPa as against the 262 MPa yield stress). Nevertheless, at very high loads shear failure modes limit the flexural loads that the specimens can bear for long periods of time. The superiority of the 7.5 wt % system compared to the 5 wt % system was again demonstrated. The 7.5 wt % specimen sustained a 415 MPa load for over 100 h without deterioration in properties, whereas the 5 wt % specimen was not.

For the 2.5 wt % glass-doped system the microyield point stress is 449 MPa. The static fatigue experiment was conducted at 520 MPa. Because this load exceeded the capability of the static fatigue apparatus, the specimen width was decreased from the previous 6.4 mm to 3.8 mm. This created several set-up problems and concerns about twisting loads applied to the specimens. At the 520 MPa load the specimen broke in less than 1 h, and failed in tension. This failure indicates that fluidity of the glass is not sufficient to blunt the cracks at this low percentage of glass content.

The 900 °C experiments clearly show that the 7.5 wt % glass-doped system is superior to that of 5 or 2.5 wt % systems.

3.2.2.3. *Experiments at 800 °C.* As Table IX indicates, the 7.5 wt % glass-doped system has a microyield point of 359 MPa at 800 °C. Static fatigue was carried out at 428 and 497 MPa. There was no failure at the 428 MPa stress level for 110 h, with a retained strength of 760 MPa and ultimate strain of 0.64%, and no deterioration in properties. At the 497 MPa stress

TABLE VII Results of static fatigue experiments at 1000 °C

Glass doping level (wt %)	σ_{MY} (MPa)	σ_T (MPa)	Test time (h)	Test result	Retained strength (MPa) and strain (%)
2.5	145	276	108	No failure	794 (0.7)
			108	No failure	814 (0.65)
			110	No failure	924 (0.72)
5.0	138	276	105	No failure	760 (0.7)
			110	No failure	814 (0.68)
			110	No failure ^a	656 (0.44)
7.5	131	276	108	No failure	760 (0.7)
			108	No failure	745 (0.64)
			110	No failure	794 (0.62)

^a Shear crack.

TABLE VIII Results of static fatigue experiments at 900 °C

Glass doping level (wt %)	σ_{MY} (MPa)	σ_T (MPa)	Test time (h)	Test result	Retained strength (MPa) and strain (%)
2.5	448	518	1	Failed	—
5.0	262	345	126	No failure	828 (0.7)
			21	Shear failure	
7.5	262	415	108	No failure	793 (0.72)

TABLE IX Results of static fatigue experiments at 800 °C

Glass doping level (wt %)	σ_{MY} (MPa)	σ_T (MPa)	Test time (h)	Test result	Retained strength (MPa) and strain (%)
2.5	435	504	1	Failed	—
5.0	435	504	1	Failed	—
7.5	359	428	108	No failure	760 (0.64)
		504	24	Shear crack formation and failure	

level, however, the specimen failed after 21 h, while shear crack formation below a support point which led to the failure was clearly evident. The calculated maximum shear stress for the test configuration is about 35 MPa, which is probably close to the shear strength of the specimen at the temperature which causes such failures. For both the 2.5 and 5 wt % systems the microyield stress is 435 MPa. At a 497 MPa load in static fatigue, both specimens failed in tension after 1 h.

Thus even at 800 °C the 7.5 wt % glass-doped system is superior to the 2.5 and 5 wt % systems. At 497 MPa load the 7.5 wt % system failed in shear after 24 h, whereas the other systems failed in 1 h.

The static fatigue experiments carried out at three temperatures with the three systems confirm that 7.5 wt % glass-doped system is superior to the other two. Static fatigue and retained strength experiments

clearly point out the superiority of the glass-doped systems over the conventional systems. Stresses which were 2 to 3 times the microcrack or microyield stress could be applied without sample failure for long periods of time (> 100 h) at temperatures of 800 to 1000 °C where the oxidation-embrittlement problem is most severe.

3.3. Effect of dopant glass composition and the glass–ceramic phase on composite performance

The effect of dopant glass composition on composite performance was determined by removal of potassium and changing the B_2O_3/SiO_2 ratio in the glass. The experiments were done with the cordierite glass ceramic phase combined with 2.5 and 5 wt % glass dopant levels. An anorthite glass–ceramic phase at 5 wt % glass doping level, with the variations in dopant glass composition mentioned above, was also evaluated. Table X shows the properties of the cordierite composite system with 5 wt % glass doping. The results (and those in Table XI below) are different from those in Tables IV, V and VI for the same system because improved processing was used for the later work. In Table X, ultimate strengths at all temperatures decline significantly as the glass is stiffened by removing K_2O or increasing the ratio of SiO_2/B_2O_3 . The ultimate failure strains at 1000 °C also decrease with increasing stiffness of dopant glass. A similar pattern is seen with the 2.5 wt % glass-doped com-

TABLE X Effect of variation of dopant glass stiffness on composite properties (cordierite–5 wt % glass)

Composite No.	Matrix	Test temperature (°C)	σ_{MCY} (MPa)	ϵ_{MCY} (%)	σ_{ULT} (MPa)	ϵ_{ULT} (%)
1	5% KBS glass; $SiO_2/B_2O_3 = 80/20$	25	524	0.33	911	0.77
		1000	193	0.19	821	0.96
		1200	124	0.16	725	1.2
2	5% glass, K_2O removed; $SiO_2/B_2O_3 = 80/20$	25	497	0.32	635	0.49
		1000	207	0.19	731	0.79
		1200	90	0.13	621	1.23
3	5% glass, K_2O_3 removed; $SiO_2/B_2O_3 = 85/15$	25	462	0.33	821	0.72
		1000	152	0.15	345	0.40
		1200	69	0.09	531	0.91

TABLE XI Effect of variation of dopant glass stiffness on composite properties (cordierite–2.5 wt % glass)

Composite No.	Matrix	Test temperature (°C)	σ_{MCY} (MPa)	ϵ_{MCY} (%)	σ_{ULT} (MPa)	ϵ_{ULT} (%)
1	2.5% KBS glass; $SiO_2/B_2O_3 = 80/20$	25	440	0.28	862	0.70
		1000	214	0.23	655	0.73
		1200	221	0.34	621	1.08
2	2.5% BS glass, K_2O removed; $SiO_2/B_2O_3 = 85/15$	25	495	0.31	931	0.98
		1000	297	0.25	410	0.35
		1200	90	0.13	517	0.81
3	2.5% BS glass, K_2O_3 removed; $SiO_2/B_2O_3 = 85/15$	25	421	0.27	718	0.63
		1000	290	0.25	531	0.53
		1200	97	0.12	483	0.80

TABLE XII Effect of variation of dopant glass stiffness on composite properties (anorthite-5 wt % glass)

Composite No.	Matrix	Test temperature (°C)	σ_{MCY} (MPa)	ϵ_{MCY} (%)	σ_{ULT} (MPa)	ϵ_{ULT} (%)
1	Anorthite + 5% KBS glass; SiO ₂ /B ₂ O ₃ = 80/20	25	310	0.25	566	0.48
		1000	310	0.29	317	0.31
		1200	110	0.16	455	0.74
2	Anorthite + 5% BS glass; SiO ₂ /B ₂ O ₃ = 80/20 (K ₂ O removed)	25	435	0.32	552	0.44
		1000	235	0.21	372	0.34
		1200	104	0.14	455	0.62
3	Anorthite + 5% BS glass; SiO ₂ /B ₂ O ₃ = 80/20 (K ₂ O removed)	25	400	0.30	635	0.55
		1000	400	0.34	428	0.36
		1200	117	0.17	511	0.80

posites behaving in a similar manner, as shown in Table XI. With increasing glass stiffness, ultimate strengths generally decrease at elevated temperature.

As discussed above, it is preferable to have as stiff a dopant glass as possible without sacrificing the oxidation-embrittlement resistance of the composites. Stiffer glasses also allow higher-temperature use capability and improved creep resistance. A complete optimization of processing parameters and detailed characterization of the composites is necessary to choose the best composition for a given application. At this point compositions have been evaluated based only on MOR data. On that basis a dopant glass composition with K₂O and an 80/20 ratio for SiO₂/B₂O₃ appears optimum for cordierite-based systems.

The mechanical properties of the matrix glass-ceramic phase are very important in determining composite performance. The higher the matrix modulus the lower is the critical aspect ratio, and thus the higher the load transfer to a whisker with a given aspect ratio and modulus. If another glass-ceramic phase with a significantly lower modulus is substituted for cordierite, the mechanical properties should be lower. For such a glass-ceramic phase the composite performance is expected to improve with increasing stiffness of the dopant glass. To confirm these conclusions, an anorthite-based system was evaluated. Anorthite has a significantly lower modulus (96 GPa) compared to that of cordierite (130 GPa).

For samples with 5 wt % glass doping of the matrix, composite properties are summarized in Table XII. The dopant glass composition was varied in accordance with that of the cordierite system. In comparing the properties of composite 1 (anorthite) in Table XII and composite 1 (cordierite) in Table X, ultimate strengths of the anorthite-based composition are seen to be substantially lower at all temperatures. As the stiffness of dopant glass increases, the composite performance improves significantly. Composite 3 with the stiffest glass has the best properties. This result is contrary to the result obtained with the cordierite-based systems in Table X, where a stiffer glass resulted in worse properties because of the reasons mentioned above.

Thus the composite performance is affected by the modulus of the glass-ceramic phase. It is noted, however, that the chemical differences in compositions

which engender differences in bond strength etc. have not been considered.

4. Summary

From this preliminary work, glass-doped ceramic matrices hybridized with silicon carbide whiskers yield composites with significantly improved high-temperature properties over those of conventional glass-ceramic matrix composites. These composites can withstand stresses substantially above the microcrack or microyield stress for long periods of time (> 100 h) at elevated temperatures in air. No strength degradation is observed during the static fatigue experiments.

It has been shown that various factors, including the modulus of the glass-ceramic phase and the relative stiffness of the dopant glass affect the composite performance significantly. These parameters must be studied in detail to obtain a clear understanding of composite mechanics.

Acknowledgements

J. F. Mach and the Composite Fabrication Center staff at Sullivan Park (Corning) fabricated the composites. K. P. Reddy, Eugene Nowlan and Bill Vann carried out the mechanical testing of composites. John Bartoo and Dave Pickles helped in SEM and TEM characterization.

References

1. K. M. PREWO and J. J. BRENNAN, *J. Mater. Sci.* **15** (1980) 463.
2. J. J. BRENNAN and K. M. PREWO, *ibid.* **17** (1982) 2871.
3. K. CHYUNG, M. P. TAYLOR and R. L. STEWART, presented at 8th Annual Meeting of the American Ceramic Society, Cincinnati, May 1985.
4. R. L. STEWART, K. CHYUNG, M. P. TAYLOR and R. F. COOPER, in "Fracture Mechanics of Ceramics", Vol. 7, edited by R. C. Bradt, D. P. H. Hasselman, A. G. Evans and F. F. Lange (Plenum, 1986).
5. K. P. GADKAREE, K. C. CHYUNG and M. P. TAYLOR, *J. Mater. Sci.* **23** (1988) 3711.
6. R. W. RICE, US Patent 4642271.
7. K. CHYUNG and S. B. DAWES, *J. Mater. Sci. Eng.* **A162** (1993) 27.
8. K. P. GADKAREE, *J. Mater. Sci.* **26** (1991) 4845.

Received 21 January
and accepted 8 October 1993